frontiers | Frontiers in Materials

TYPE Original Research
PUBLISHED 30 October 2024
DOI 10.3389/fmats.2024.1501505

OPEN ACCESS

EDITED BY
Chunguang Yang,
Chinese Academy of Sciences (CAS), China

REVIEWED BY
Xiao Lin,
Soochow University, China
Chun-Dong Xue,
Dalian University of Technology, China

*CORRESPONDENCE
Dewei Zhao,
zhaodewei2016@163.com

RECEIVED 25 September 2024
ACCEPTED 17 October 2024
PUBLISHED 30 October 2024

CITATION
Liu G, Wei X, Li J, Zhai Y, Zhang J, Jin M, Guan T and Zhao D (2024) Hydrogel composition and mechanical stiffness of 3D bioprinted cell-loaded scaffolds promote cartilage regeneration.
Front. Mater. 11:1501505.
doi: 10.3389/fmats.2024.1501505

Hydrogel composition and mechanical stiffness of 3D bioprinted cell-loaded scaffolds promote cartilage regeneration

Ge Liu[1,2], Xiaowei Wei[2], Junlei Li[2], Yun Zhai[1], Jingrun Zhang[2], Ming Jin[2], Tianmin Guan[1] and Dewei Zhao[1,2]*

[1]School of Mechanical Engineering, Dalian Jiaotong University, Dalian, China, [2]Department of Orthopedics, Affiliated Zhongshan Hospital of Dalian University, Dalian, China

Objective: To investigate the impact of different component ratios and mechanical stiffness of the gelatin-sodium alginate composite hydrogel scaffold, fabricated through 3D bioprinting, on the viability and functionality of chondrocytes.

Methods: Three different concentrations of hydrogel, designated as low, medium, and high, were prepared. The rheological properties of the hydrogel were characterized to optimize printing parameters. Subsequently, the printability and shape fidelity of the cell-loaded hydrogel scaffolds were statistically evaluated, and the chondrocyte viability was observed. Dynamic mechanical analysis was conducted to measure the modulus, thereby assessing the scaffold's stiffness. Following a 21-day culture period, RT-PCR, histological staining, and immunostaining were employed to assess chondrocyte activity, chondrosphere aggregates formation, and cartilage matrix production.

Results: Based on rheological analysis, optimal printing temperatures for each group were determined as 27.8°C, 28.5°C, and 30°C. The optimized printing parameters could ensure the molding effect of the scaffolds on the day of printing, with the actual grid area of the scaffolds was close to the theoretical grid area. And the scaffolds exhibited good cell viability (93.24% ± 0.99%, 92.04% ± 1.49%, and 88.46% ± 1.53%). After 7 days of culture, the medium and high concentration groups showed no significant change in grid area compared to the day of printing ($p > 0.05$), indicating good morphological fidelity. As the hydrogel's bicomponent ratio increased, both the storage modulus and loss modulus increased, while the loss factor remained relatively constant. The highest number of chondrocytes-formed chondrosphere aggregates in the medium concentration group was observed by light microscopy. RT-PCR results indicated significantly higher expression levels of chondrogenic genes SOX9, Agg, and Col-II in the low and medium concentration groups compared to the high concentration group ($p < 0.05$). Histological staining results showed that the middle concentration group formed the highest number of typical cartilage lacunae.

Conclusion: The aforementioned results indicate that in 3D bioprinted cell-loaded GA-SA composite hydrogel scaffolds, the scaffolds with

the composition ratio (10:3) and mechanical stiffness (~155 kPa) exhibit sustained morphological fidelity, effectively preserve the hyaline phenotype of chondrocytes, and are more conducive to cartilage regeneration.

KEYWORDS

gelatin, sodium alginate, hydrogel, chondrocyte, bioprinting, mechanical stiffness

1 Introduction

Articular cartilage has a unique physiological structure characterized by a lack of vascularity and nutrient supply. Once damaged, its ability of self-repair and regeneration is severely limited (Armiento et al., 2019; Liu et al., 2024). Natural degeneration or trauma-induced cartilage defects can lead to secondary osteoarthritis, causing joint pain and seriously affecting patients' quality of life (Katz et al., 2021; Salzmann et al., 2021). Current clinical treatment options for cartilage defects include debridement, microfracture, autologous/allogeneic cartilage transplantation, and autologous chondrocyte transplantation (Yasui et al., 2017; Redondo et al., 2018; Gao et al., 2019; Na et al., 2019). Although these treatments may enhance joint function and alleviate pain, they often result in cartilage fibrosis. In addition, problems such as donor shortage, immune rejection, and poor integration severely limit their widespread application (Gobbi et al., 2020; Zhou et al., 2023). Therefore, articular cartilage damage is one of the most challenging clinical problems in orthopedics.

The development of tissue engineering offers a solution to the challenge of cartilage damage. Ideal tissue-engineered cartilage constructs should mimic the native extracellular matrix (ECM), encapsulate cells, and not only fill and maintain the defect space as new tissue grows but also integrate with the surrounding native tissue (Caddeo et al., 2017; Fu et al., 2021). 3D bioprinting facilitates the creation of scaffolds that can achieve ideal tissue-engineered structures by simultaneously extruding living cells and biomaterials (Abdollahiyan et al., 2020; Lafuente-Merchan et al., 2022). Scaffolds formed by bioprinting can be personalized and simulate natural tissue structures containing cells (Daly and Kelly, 2019; Zhang et al., 2019). Therefore, materials suitable for bioprinting are required to be both biocompatible and printable. Hydrogels consist of cross-linked hydrophilic polymers that can absorb large amounts of water without dissolving, and are often used as bioinks for bioprinting in cartilage tissue engineering due to their low cytotoxicity and structural similarity to natural ECM (Chung et al., 2013; Kyburz and Anseth, 2015). Biochemical components of biomaterials in direct contact with cells plays a crucial role in regulating cell behavior (Seo et al., 2019; Liu Y. et al., 2023).

In this study, we used two well-characterized and frequently used natural hydrogel materials, sodium alginate (SA) and gelatin (GA). SA is a naturally occurring block copolymer consisting of a combination of β-D-mannuronate (M) and α-L-guluronate (G) polymer blocks (Lee and Mooney, 2012). It is an attractive hydrogel for bioprinting applications because its printability can be easily modified by varying the polymer density and cross-linking with the addition of calcium chloride ($CaCl_2$) (Duan et al., 2013). GA is the hydrolyzed product of collagen and contains a hydrophilic component of the arginine-glycine-aspartic acid (RGD) sequence that promotes chondrocyte proliferation and differentiation (Skardal and Atala, 2015; Morshedloo et al., 2020). Thus, GA-SA composite hydrogels with adjustable mechanical properties are an attractive bio-extrusion molding bioink due to their good cytocompatibility, printability, and ability to maintain structure during long-term culture (Giuseppe et al., 2018; Henrionnet et al., 2020; Wang et al., 2023). In addition, the mechanical stiffness of hydrogels has also been shown to influence cellular function and fate. For example, in gelatin methacrylate-hyaluronic acid methacrylate (GelMA-HAMA) hydrogels with a stiffness ranging from 30 to 60 kPa, chondrocytes exhibited higher expression of type II collagen, which favors cartilage formation (Martyniak et al., 2022). Liu et al. fabricated gradient hydrogels with adjustable stiffness by varying the concentration and volumes of polyethylene glycol (PEG) precursor solution, and chondrocytes produced more cartilage matrix in a hydrogel environment with Young's modulus of 20–40 kPa (Liu et al., 2021). Bachmann et al. (2020) demonstrated that fibrin hydrogel with Young's modulus of 30 kPa can best guide chondrocyte redifferentiation to form a native-like morphology and induce the synthesis of physiological ECM components, such as glycosaminoglycans (sGAG) and type II collagen. Therefore, the optimal mechanical stiffness that is conducive to the formation of a cartilage matrix differs for chondrocytes in different hydrogel compositions.

However, the appropriate mechanical stiffness that favors the maintenance of the chondrocyte phenotype in 3D bioprinted GA-SA composite hydrogel scaffolds remains unclear. Therefore, in order to study the effect of different bioprinted chondrocyte-loaded scaffold stiffness on cell viability and cartilage matrix formation, we established a complete standard printing optimization protocol by comprehensively evaluating the printing molding effect and chondrocyte activity of cell-loaded hydrogel scaffolds. On this basis, the optimal composition and mechanical stiffness of hydrogel suitable for cartilage regeneration were determined based on the storage modulus of the hydrogel and the results of cartilage matrix formation. From the perspective of the composition and mechanical stiffness of biomaterials, exploring their impact on chondrocyte phenotype and function will enable us to better design regenerative biomaterials for cartilage tissue engineering, and such cartilage scaffolds will also have a more favorable clinical potential.

2 Materials and methods

2.1 Consumables, equipment, and supplies used

GA, SA, $CaCl_2$ were purchased from Sigma-Aldrich, United States. Fetal bovine serum (FBS), phosphate buffered solution (PBS),

DMEM/F12 medium, streptomycin and penicillin, and trypsin were purchased from Gibco, United States. CCK-8 kit, Calcein/PI double staining kit for live and dead cells were purchased from Tongren, Japan. Chondrocyte complete culture medium was purchased from Punuosai, China. Primer synthesis, Trizol reagent, PrimeScript reverse transcription kit, and SYBR Green PCR Master mix kit were purchased from TaKaRa, Japan. Type I collagen antibody and type II collagen antibody were purchased from Abcam, United States.

Bio-3D printer (Jienuofei, China), enzyme labeler (Biotek, United States), inverted fluorescence microscope (Olympus, Japan), rheometer and dynamic thermo-mechanical analyzer DMA (TA, United States), polymerase chain reaction analyzer (ABI, United States).

2.2 Isolation and culture of rat chondrocytes

Based on methods reported in the mentioned paper (Zhang et al., 2017), Chondrocytes were isolated from the knee cartilage of 1-month-old Sprague Dawley (SD) rats. Briefly, the cartilage was cut into small pieces. They were washed three times with PBS. Subsequently, the cartilage tablets were digested with collagenase type II (0.1%) for 8 h in a 37°C water bath. After 5-min centrifugation at 200 *g*, the mixed cartilage and chondrocytes were suspended in DMEM/F12 with 10% FBS. Chondrocytes were then inoculated in culture flasks and cultured at 37°C in a 5% CO_2 incubator and passed through passage 3 to obtain purified chondrocytes.

2.3 Preparation of composite hydrogel ink

GA and SA were weighed according to the mass fraction (W/V) and sterilized by UV light for 30 min before use, then dissolved in sterile deionized water, stirred homogeneously, and incubated at 42°C for 12 h. Then, centrifuged to remove air bubbles for subsequent experimental detection. Alternatively, the composite hydrogel was mixed with chondrocyte suspension (number of cells: hydrogel = $2^{*}10^{6}$ cells:1 mL) and incubated at 37°C for use. The composite hydrogels were divided into 3 groups according to different mass fractions, recorded as GA8SA2, GA10SA3, and GA15SA5, respectively.

2.4 Cell proliferation test of composite hydrogel

Three groups of GA-SA composite hydrogels were extracted with a simple culture medium and a concentration of 0.1 g/mL in a 37°C thermostat for 24 h, and 10% FBS and 1% penicillin/*streptomyces* were added to the extract of each group of materials. Cells were seeded into the wells of a 96-well plate at a number of 1×10^{4}/well. The hydrogel extract of each group was added to the experimental group, and the complete culture medium was added to the control group. The detection time points are 1 d, 3 d, 5 d, and 7 d. On the detection day, the extracted culture solution was first removed from the well plate and rinsed three times with PBS. Then, 100 μL fresh medium and 10 μL CCK8 solution were added to each well. After incubation for 2 h, the absorbance value of each well was measured at 450 nm.

2.5 Effect of cross-linking conditions on cell viability in composite hydrogel

Chondrocyte-loaded hydrogel ink was extruded into 48-well plates and cross-linked with $CaCl_2$ solution. The concentrations of $CaCl_2$ solution were 50 mM, 100 mM, 200 mM, 300 mM, 400 mM, and 500 mM, and the cross-linking times were 10 min, 20 min, and 30 min, respectively. The Calcein/PI live and dead cell double-staining kit was used to stain chondrocytes. Green fluorescence for live cells and red fluorescence for dead cells, which were observed by inverted fluorescence microscope. Five different areas in the Figures were arbitrarily selected for each sample for average quantitative analysis, and the figures were counted by color classification using Image Pro Plus 6.0 software, and the cell survival rate was calculated according to the following formula: total number of live cells/(total number of live cells + total number of dead cells) × 100%. This method was also used for cell viability detection in chondrocyte-loaded hydrogel scaffolds.

2.6 Rheological testing of composite hydrogels

An AR 2000ex rotational rheometer was used to test the rheological properties of the hydrogel ink. The test uses the flat plate mode, using a hardened aluminum parallel plate with a diameter of 60 mm as the measurement fixture. The experimental setting gap is 1,000 μm, the strain is controlled at 0.1%–3%, and the dynamic frequency is 1.5 Hz. Test temperature is 0°C–40°C. Parameters such as composite viscosity (η^{*}), storage modulus (G'), and loss modulus (G'') were recorded with temperature and time.

2.7 3D bioprinting of composite hydrogel scaffolds

Both simple composite hydrogel scaffolds and chondrocyte-loaded hydrogel scaffolds were prepared by a bio-3D printer. A printing needle with an inner diameter of 0.42 mm was used to print according to the specimen model designed by the software. In order to test cell viability, double-layer mesh scaffolds were printed using an alternating superposition method of 0°–90°, while the optimal printing parameters were determined based on the experimental method of mesh area measurement. Printed cylindrical scaffolds (diameter 8 mm*height 6 mm) were used for dynamic mechanical analysis (DMA) testing, prolonged light microscopy observation, pathological staining, immunostaining, and RT-PCR assays.

2.8 DMA testing of chondrocyte-loaded hydrogel scaffolds

Before testing, the discs were equilibrated to room temperature, and the width and height were measured with calipers. Unlimited

TABLE 1 Primers used for the qRT-PCR analysis.

Gene	Primer sequence	Product size (bp)
SOX9	F:caagttccccgtctgcatc	111
	R:tgcggcttgttcttgctc	
Agg	F:cctcaccatcccctgctactt	119
	R:gcaccacctccttctccttg	
Col-II	F:ctcaagtccctcaacaaccaga	123
	R:ccagtagtctccgctcttcca	
Col-I	F:tggtgaagcaggcaaacct	87
	R:aaacctctctcgcctcttgct	
GAPDH	F:ttgtgatgggcgtgaacc	127
	R:ccctccacgatgccaaa	

uniaxial compression tests were performed using DMA. Strain was tested at 1 Hz (10%, 100 μm). All tests were done at room temperature and measurements were taken for 30 min. G′, G″ and loss factor (Tan δ) were detected and the final values were calculated based on the average of 20–30 min during the curve plateau.

2.9 Prolonged culture observation of chondrocyte-loaded hydrogel scaffolds

The printed chondrocyte-loaded hydrogel scaffolds were placed in a 24-well plate and cultured with chondrocyte complete medium up to 21 d. Among them, observation was carried out with an inverted phase contrast microscope at 7 d, 14 d, and 21 d. The numbers of chondrosphere aggregates were analyzed using ImageJ software and expressed as Numbers/mm^2.

2.10 RT-PCR to detect the expression of chondrogenic-related genes

After the three groups of chondrocyte-loaded hydrogel scaffolds were cultured for 21 d, total RNA was extracted by Trizol reagent method, and cDNA was synthesized by reverse transcription, followed by RT-PCR reaction. The relative mRNA expression of chondrogenic-related genes was calculated according to the $2^{-\Delta\Delta Ct}$ method. The primer sequences are shown in Table 1.

2.11 Histological and immunostaining analysis of chondrocyte-loaded hydrogel scaffolds

Three groups of hydrogel-chondrocyte scaffolds were cultured for 21 d, fixed with 40 g/L paraformaldehyde, embedded in paraffin wax, and sectioned. The thickness of the sections was 2 μm. Toluidine blue staining was performed for observation. Meanwhile, the sections were treated with trypsin working solution for 15 min, blocked with serum sealing solution for 15 min, washed with PBS, and incubated with diluted primary antibodies against type I and type II collagen overnight, respectively. After which the secondary antibodies were incubated for 30 min, stained with DAB to develop the color, and the expression of collagen was observed under the microscope. The intensity of the positive immunohistochemical reaction was analyzed using ImageJ software and expressed as an AOD (IOD/Area) value.

2.12 Statistical methods

Statistical analysis was performed using SPSS 22.0 software. Data were presented as mean ± standard deviation. Comparison between two groups was performed using t -test. Comparison of means among multiple groups was performed using ANOVA. Single-factor analysis of variance was used. Tukey test was used for pairwise comparison. $p < 0.05$ was used to indicate that the difference was statistically significant.

3 Results

3.1 Cell proliferation analysis and cross-linking conditions optimization of composite hydrogels

The statistical results of CCK8 assay showed that the number of cells in each group increased with the prolongation of culture time. And compared with the control group, the absorbance values of chondrocytes cultured with the three groups of GA-GA composite hydrogel extracts after 1, 3, 5, and 7 d were not significantly different ($p > 0.05$). It indicated that the GA-GA composite hydrogel had good biocompatibility and was non-toxic to chondrocytes (Figure 1A). The chondrocyte-loaded composite hydrogels were treated with $CaCl_2$ at concentrations of 50 mM, 100 mM, 200 mM, 300 mM, 400 mM, and 500 mM for durations of 10 min, 20 min, and 30 min, respectively. The results of the live-dead cell staining showed that the cell viability decreased with increasing $CaCl_2$ concentration and cross-linking duration, but within 50 mM, 100 mM, and 200 mM treatment for 30 min, the cell viability remained above 90% (Figures 1B,C). Therefore, the cross-linking agent concentration was determined to be 200 mM, and the cross-linking duration was set to 30 min in this experiment.

3.2 Rheological performance analysis of composite hydrogel inks

This study investigated the rheological properties of GA-SA composite hydrogel inks with three different concentrations. The comparison of temperature rise and fall curves revealed that the rheological behavior of GA-SA hydrogel ink was

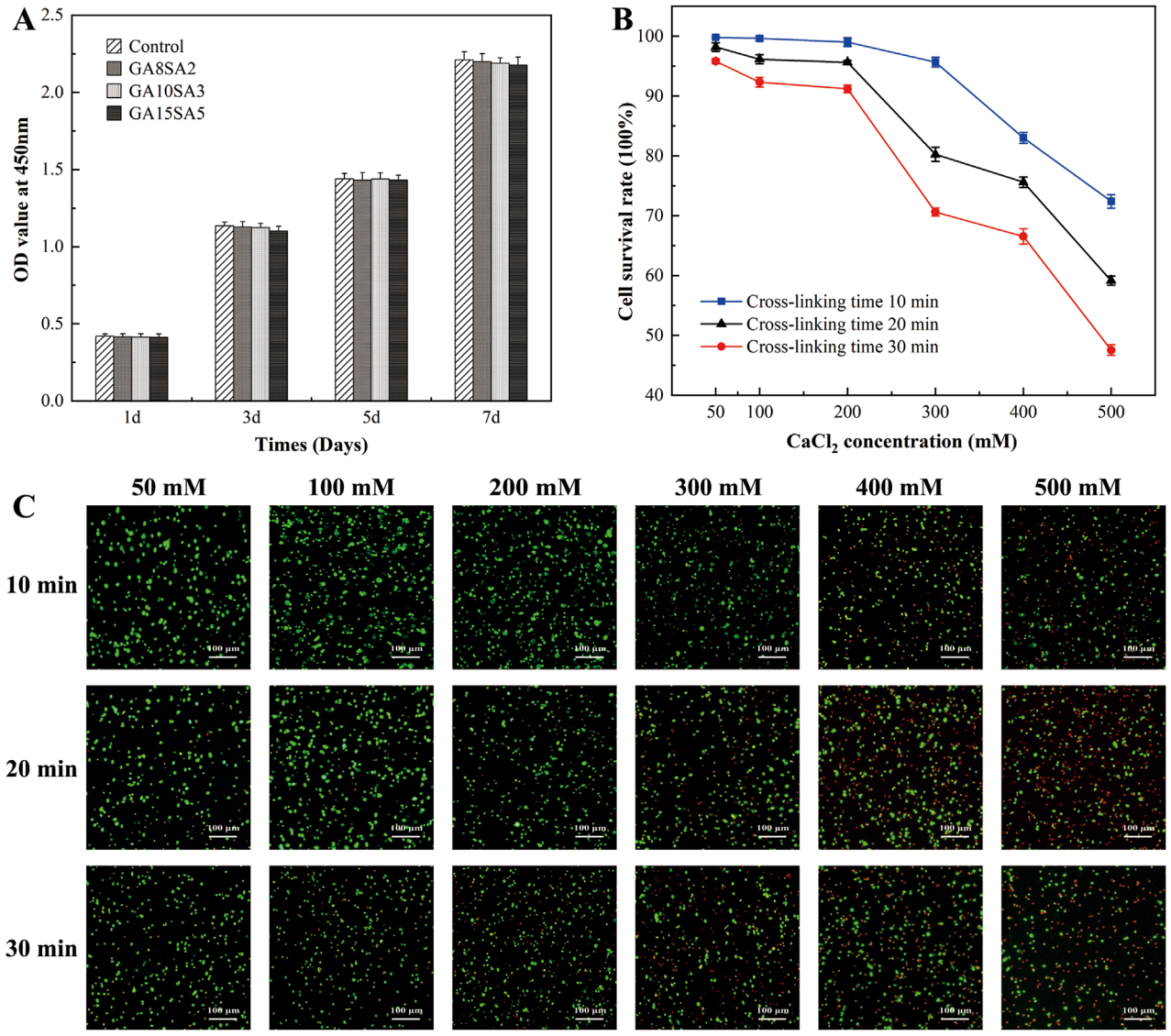

FIGURE 1
Effect of hydrogel and its cross-linking conditions on chondrocyte activity. **(A)** CCK8 detection to the proliferation of chondrocytes treated with different concentrations of hydrogel extracts. **(B)** Live-dead staining of chondrocytes in hydrogels treated with different $CaCl_2$ crosslinker concentrations and time. **(C)** Statistical graph of cell survival rate by live-dead staining results.

inconsistent during the sol (temperature rise) and gel (temperature fall) processes, with the sol temperature being higher than the gel temperature (Figures 2A–C). The sol/gel intersection temperature of each group were shown in Table 2. As the concentration of the GA-SA component increased, both the sol/gel transition temperatures increased. Such changing rules provided a certain reference for selecting the printing temperature of hydrogel ink.

After that, the time-scan curves of three groups of GA-SA inks at different test temperatures were tested. The test temperatures were the sol/gel intersection temperatures of each group of hydrogel inks and their intermediate temperatures, respectively (Table 2). The time response variation rules of the three groups of GA-SA inks were consistent, that is, at the gel intersection temperature, G′ was larger than G″, and the inks were in a completely gel state; at the sol intersection temperature, G″ was larger than G′, and the inks were in a completely sol state; at the intermediate temperatures, G″ was larger than G′ first, and then G′ was larger than G″ after that, but the values of G″ and G′ were always close to each other, indicating that the ink is always in the transition state of gel-sol. With a semi-fluid nature, it may be more conducive to hydrogel print molding (Figures 2D–F).

Then, $2^{*}10^{6}$/mL chondrocytes were added to the hydrogel ink system for testing. At the intermediate temperatures of the three groups of hydrogel inks, the addition of chondrocytes barely changed the viscosity of the hydrogel ink, that is, it had little effect on the rheological properties of the hydrogel (Figures 2G–I). Therefore, it can be surmised that chondrocytes with a density of $2^{*}10^{6}$/mL can be used for printing cell-loaded hydrogel scaffolds.

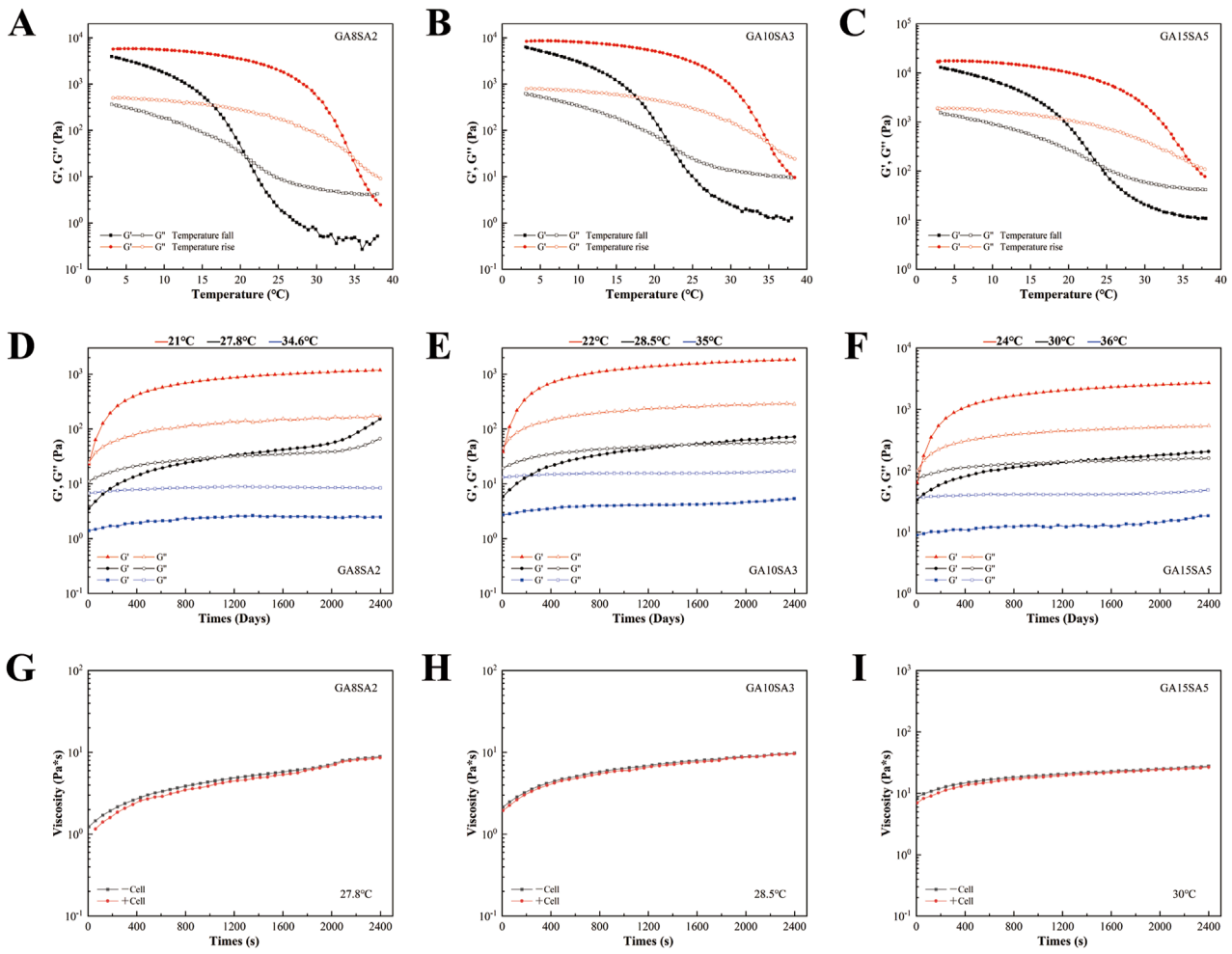

FIGURE 2
Rheological characterization of hydrogel inks with different concentrations. **(A–C)** The temperature fall/rise comparison of different concentrations of hydrogel ink. **(D–F)** Time response of different concentrations of hydrogel ink. **(G–I)** Effect of mixing chondrocytes on the viscosity of different concentrations of hydrogel ink.

TABLE 2 The comparison results of temperature rise and fall in three groups of hydrogel bioinks.

Temperature	GA8SA2	GA10SA3	GA15SA5
Sol intersection temperature (°C)	34.6	35	36
Gel intersection temperature (°C)	21	22	24
Intermediate temperature (°C)	27.8	28.5	30

3.3 Bioprinting and cell activity assay of chondrocyte-loaded hydrogel scaffolds

Based on the previous rheological results, the suitable printing temperature can be determined as the middle temperature of the sol/gel intersection temperature. The other printing parameters of the three groups of hydrogels were optimized at this temperature. The printing pressure was between 0.12–0.17 MPa, and printing pressure increased as the hydrogel composition increased; the printing speed was 6–7 mm/s (Table 3). The results of live-dead cell staining showed that the cell survival rates of the GA8SA2 group, GA10SA3 group, and GA15SA5 group were (93.24 ± 0.99) %, (92.04 ± 1.49) %, and (88.46 ± 1.53) %, respectively (Figure 3; Table 3). The cell survival rate is greater than 85%, indicating that the cells underwent the printing process with less effect on their cellular activity. Meanwhile, statistics on the grid area of the printed scaffolds showed that the actual grid areas of the three groups of scaffolds on the day of printing were all close to the theoretical grid area (0.36 mm^2). However, after 7 d of culture, the grid area of the GA8SA2 group increased, with a statistically significant difference ($p < 0.05$); the grid area of the GA15SA5 group decreased; and the grid area of the GA10SA3 group changed little (Table 4).

TABLE 3 Statistics of suitable bioprinting parameters for chondrocyte-loaded hydrogel scaffolds.

Group	Printing temperature (°C)	Printing pressure (MPa)	Printing speed (mm/s)	Cell survival rate (%)
GA8SA2	27.8	0.12	6	93.24 ± 0.99
GA10SA3	28.5	0.13	7	92.04 ± 1.49
GA15SA5	30	0.17	6	88.46 ± 1.53

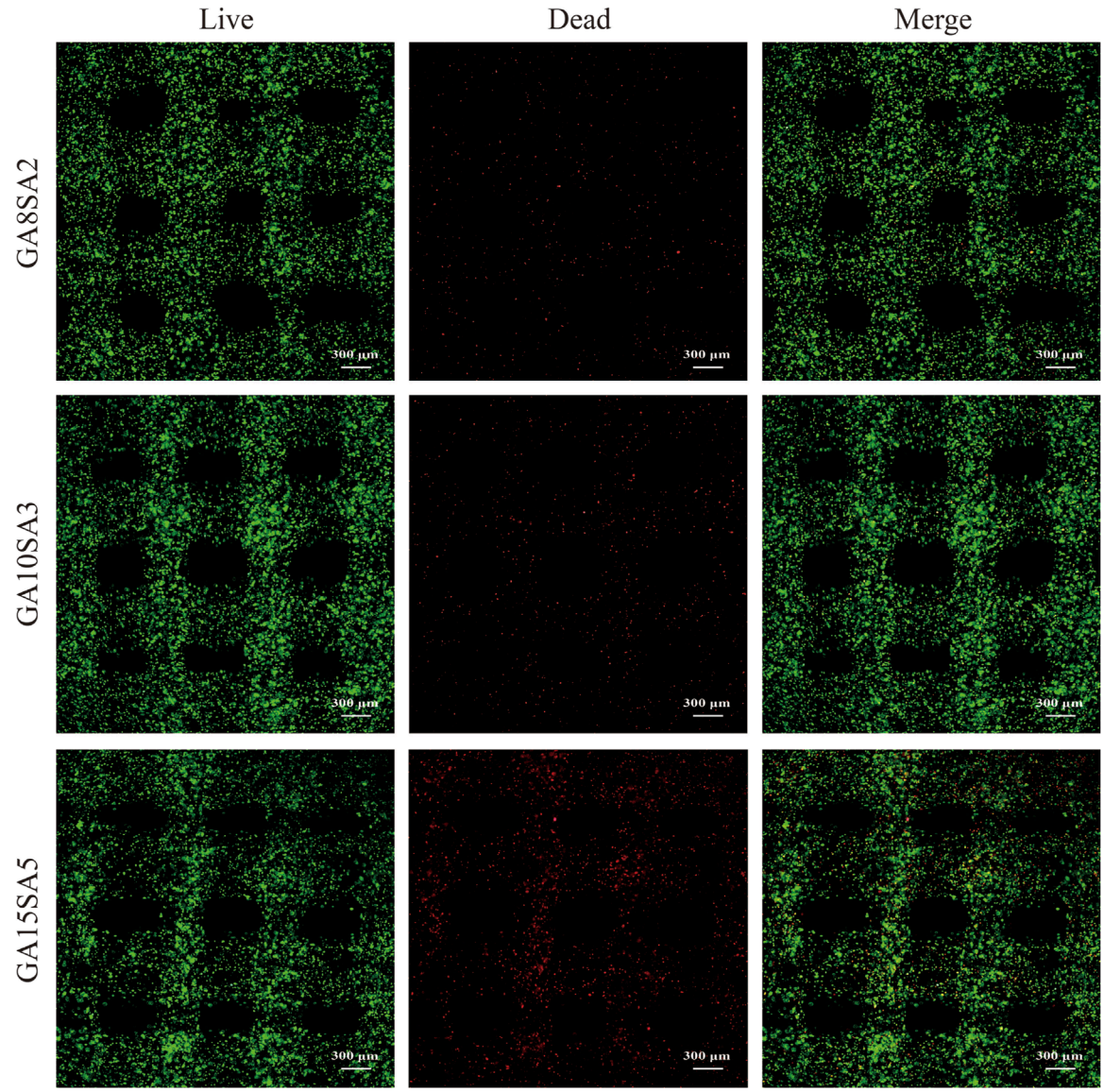

FIGURE 3
Cell activity of chondrocyte-loaded hydrogel scaffolds by bioprinting. Fluorescence figures of live -dead cells stained with chondrocytes (red: dead cells; green: live cells).

3.4 Mechanical characterization of chondrocyte-loaded hydrogel scaffolds

DMA was used to measure the modulus of the three groups of scaffolds, and the software was used to generate the G′, G″, and Tan δ of the three groups of scaffolds. Among them, the mechanical stiffness of the hydrogel scaffolds was determined by the storage modulus (G′). The G′ of the three groups of scaffolds were 81.18 ± 1.4 kPa, 155.01 ± 4.61 kPa, and 308.18 ± 9.66 kPa, respectively; the G″ were 10.67 ± 0.12 kPa, 19 ± 0.66 kPa, and 41.70 ± 1.44 kPa,

TABLE 4 Grid area statistics of chondrocyte-loaded hydrogel scaffolds.

Grid area (mm^2)	GA8SA2	GA10SA3	GA15SA5
Printing day	0.3597 ± 0.006	0.3598 ± 0.009	0.3580 ± 0.012
Culture for 7 days	0.3817 ± 0.011*	0.3559 ± 0.009	0.3484 ± 0.009
p-values	0.041	0.619	0.345

*Compared with two different time points in the same group, $p < 0.05$.

respectively; and the Tan δ were 0.130 ± 0.0008, 0.123 ± 0.0006 and 0.135 ± 0.0004, respectively (Figure 4). It was found that the proportion of hydrogel components had a significant effect on G′ and G″. G′ and G″ increased with the proportion of hydrogel components, and Tan δ did not change much.

3.5 Proliferation of chondrocytes in chondrocyte-loaded hydrogel scaffolds

In order to test the proliferation ability of chondrocytes in hydrogel scaffolds, we cultured the three groups of bioprinted chondrocyte-loaded hydrogel scaffolds for a period of up to 21 d and evaluated the culture status of chondrocytes in them. At the time of culture to 7 d, 14 d, and 21 d, they were placed under the microscope for observation. Figure 5A showed the morphology and appearance of chondrocytes and their aggregates cultured in hydrogels of the three groups. Dense aggregates of chondrospheres were formed in both the GA8SA2 and GA10SA3 groups at the time of culturing up to 14 d, and they became more and more numerous with the extension of time. At 21 d, it could be seen that the number of chondrosphere aggregates in the GA10SA3 group was significantly more than that in the GA8SA2 group. However, the GA15SA5 group never formed chondrosphere aggregates. Quantitative statistical analysis of the chondrosphere aggregates formed in each group of hydrogels. The results showed that no chondrosphere aggregates were formed in the three groups of hydrogels after 7 d of culture. The numbers of chondrosphere aggregates formed between GA10SA3 group and GA8SA2 group at 14 d and 21 d had statistical difference ($p < 0.01$) (Figure 5B). Therefore, it showed that the hydrogels with lower stiffness were more conducive to the formation of chondrosphere aggregates. And in the appropriate stiffness range, the more gelatin content, the easier to form chondrosphere aggregates.

3.6 Chondrogenic gene expression of chondrocyte-loaded hydrogel scaffolds

The chondrogenic gene expression of chondrocyte-loaded hydrogel scaffolds was verified by RT-PCR. After 21 d, the mRNA expression of SOX9, Agg, Col-II, and Col-I was analyzed in different groups (Figure 6). The mRNA expression of SOX9, Agg, and Col-II was highly significantly higher in the GA10SA3 group compared to the GA15SA5 group ($p < 0.01$), and Col-I expression was highly significantly lower compared to in the GA15SA5 group ($p < 0.01$). Similarly, SOX9 and Col-II expression was highly significantly higher in the GA8SA2 group than in the GA15SA5 group ($p < 0.01$), Agg expression was significantly higher ($p < 0.05$), and Col-I expression was highly significantly lower than in the GA15SA5 group ($p < 0.01$). These results indicated that the hydrogel scaffolds with the highest stiffness in the GA15SA5 group are unfavorable for cartilage formation. Col-II expression in the GA10SA3 group was extremely significantly higher than that in the GA8SA2 group ($p < 0.01$), Agg was significantly higher than that in the GA8SA2 group ($p < 0.05$), and there was no significant difference in SOX9 and Col-I expression. These indicated that the hydrogel scaffolds in the GA10SA3 group are more favorable for chondrocytes to maintain the hyaline phenotype.

3.7 Histologic evaluation of chondrocyte-loaded hydrogel scaffolds for cartilage formation

The three groups of hydrogels loaded with chondrocytes were cultured for 21 d for histological evaluation. Toluidine blue staining results showed that the chondrocytes within the hydrogels exhibited better growth and formed typical cartilage lacunae (Figure 7A). Specifically, the GA10SA3 group had the highest number of cartilage lacunae, followed by the GA8SA2 group, while the GA15SA5 group hardly formed any cartilage lacunae. Immunostaining for COL-II and COL-I was also performed on these three groups of hydrogel samples. The GA10SA3 and GA8SA2 groups mainly expressed collagen II rather than collagen I, whereas the GA15SA5 group showed the opposite pattern of collagen expression. Quantitative statistical analysis of collagen expression in each group of hydrogels. The results showed that compared with GA15SA5 group, GA10SA3 and GA8SA2 groups had significantly higher expression of type II collagen ($p < 0.01$) and significantly lower expression of type I collagen ($p < 0.01$) (Figures 7B,C). These results indicated that GA10SA3 and GA8SA2 groups with lower stiffness had higher expression of COL-II and were more inclined to form hyaline cartilage.

4 Discussion

GA and SA have been widely used in 3D printing as encapsulation materials for various cell types, including hematopoietic cell lines (Liu B. et al., 2023), bone marrow mesenchymal stem cells (Zhang et al., 2020), adipose stem cells (Liao et al., 2022), fibroblasts (Lee et al., 2021), endothelial cells (Kang et al., 2023), Schwann cells (Wu et al., 2020), and osteoblasts (Ojansivu et al., 2019), due to their good biocompatibility. We treated chondrocytes with different concentrations of hydrogel extracts, which did not affect cell proliferation, indicating that the GA-SA composite hydrogel has good biocompatibility with chondrocytes. The printing and molding of GA-SA scaffolds mainly relies on the cross-linking of SA and $CaCl_2$ solution to form a solid gel. For cell-containing scaffolds, the cross-linking conditions of $CaCl_2$ are particularly important. It is necessary to ensure the molding effect of the scaffold without affecting the activity of cells. Previous research had used the method of directly treating cells with

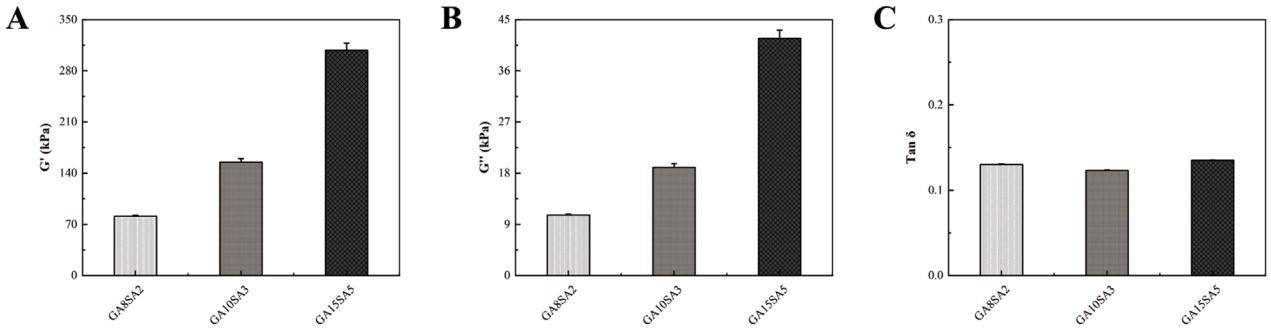

FIGURE 4
Statistics of dynamic mechanical analysis of chondrocyte-loaded hydrogel scaffolds.

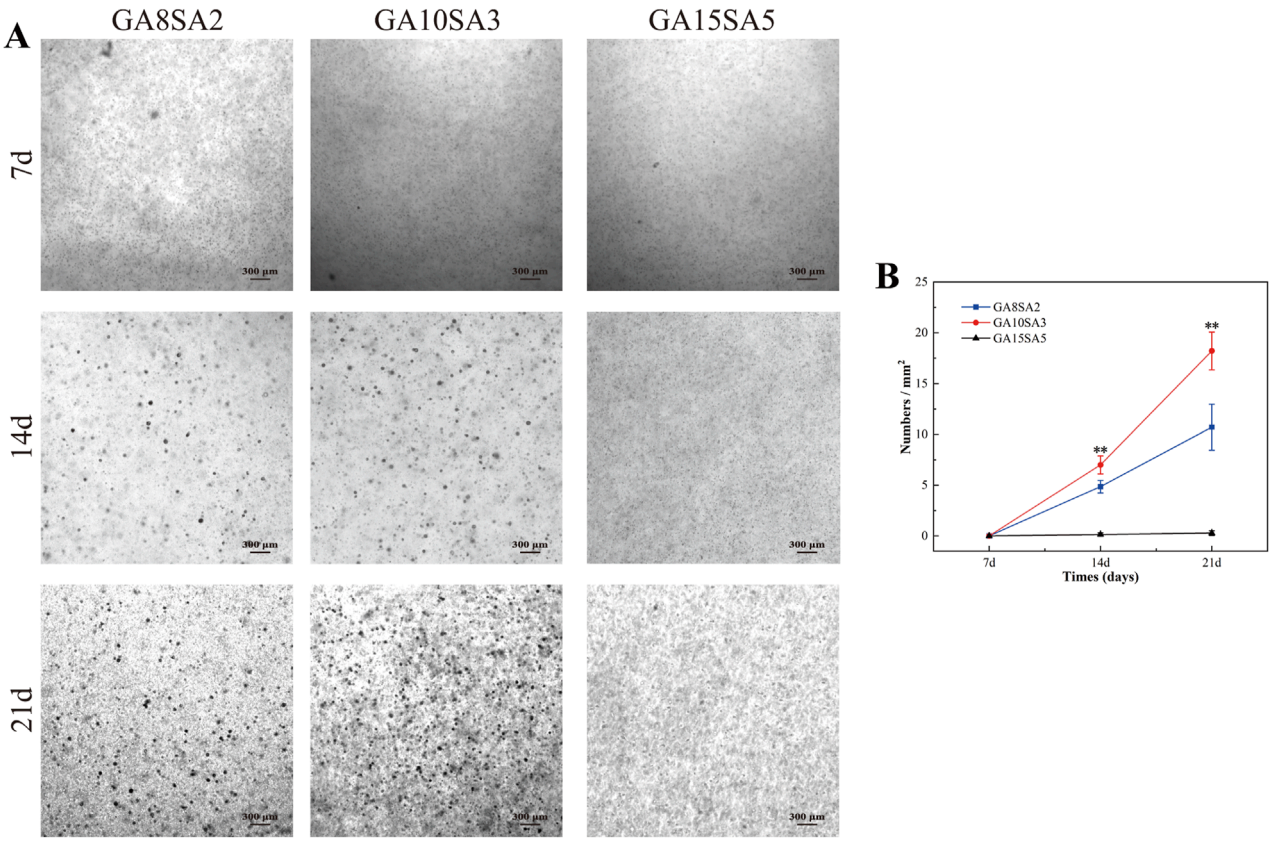

FIGURE 5
Observation and comparison of chondrosphere aggregates formed in hydrogel scaffolds at different time points. **(A)** Light microscopic observation of chondrosphere aggregates. **(B)** Quantitative analysis of the numbers of chondrosphere aggregates. Dates are represented as the mean ± SD (n = 3). Comparison between GA8SA2 and GA10SA3 groups,$^{*}p < 0.05$,$^{**}p < 0.01$.

$CaCl_2$ to choose the cross-linking conditions, and the condition of 50 mM $CaCl_2$ treatment for 5 min had less effect on the cells, but the fidelity of the scaffolds in long-term culture was poor (Wu et al., 2020). Therefore, in this study, the cell-containing hydrogel was directly treated with $CaCl_2$ to choose the optimal cross-linking conditions, which is more in line with the actual situation of scaffold molding. Based on the consideration of molding fidelity and cell activity, the final cross-linking condition was determined to be 200 mM $CaCl_2$ treatment for 30 min. At this time, the survival rate of chondrocytes was still more than 90% and the scaffolds were still able to maintain the overall morphology in the subsequent culture process.

Currently, it is still a challenge for bioprinted temperature-sensitive cell-loaded hydrogel scaffolds to achieve long-term structural stability while maintaining a high cell survival rate after printing (Zhao et al., 2015; Schwab et al., 2020; Naghieh and

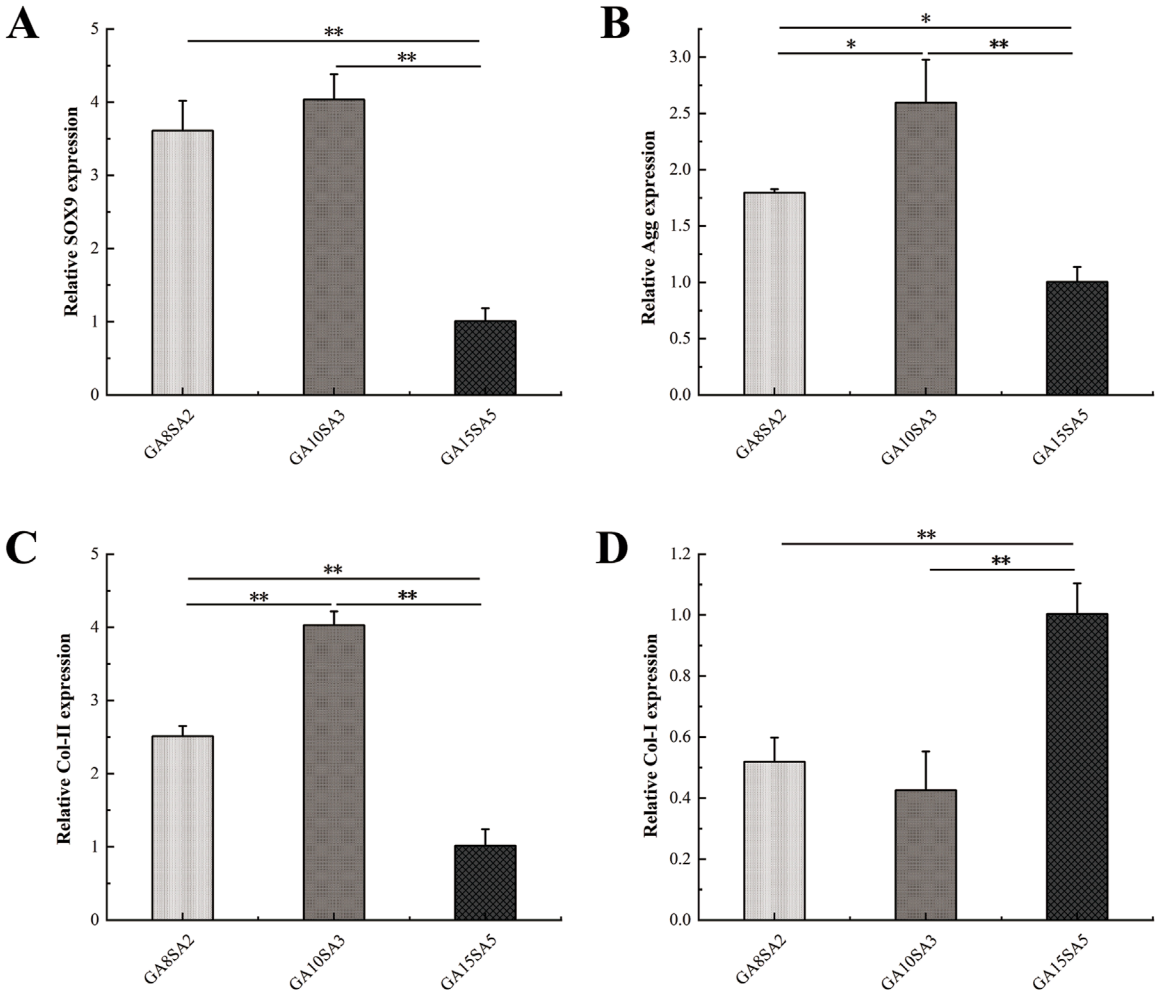

FIGURE 6
Expression of chondrogenic genes in chondrocyte-loaded hydrogel scaffolds. **(A)** SOX9 expression. **(B)** Agg expression. **(C)** Col-II expression. **(D)** Col-I expression. Dates are represented as the mean ± SD (n = 3). Comparison between groups,$^{*}p < 0.05$,$^{**}p < 0.01$.

Chen, 2021; Chen et al., 2023). Therefore, appropriate printing parameters are very important. There are also many studies on the optimization of hydrogel printing parameters (Gao et al., 2018; Rahimnejad et al., 2020; Gregory et al., 2022), but how to determine the appropriate printing temperature for temperature-sensitive hydrogel ink is often ignored. Thus, this study first characterized the sol/gel transition temperature of GA-SA hydrogels by rheological measurements, and then based on the modulus change of the ink in response to time, finally determined that the ink was in the transition state of sol-gel at the intermediate temperature of the sol/gel transition temperature, which was the most suitable for printing. And at this printing temperature, other printing parameters (printing pressure and printing speed) were adjusted to achieve good printability and cell survival. The printing and molding effect statistics of the three groups of hydrogel scaffolds showed that the actual grid area was close to the theoretical grid area (0.36 mm^2) on the day of printing. However, after 7 days of culture, the area of the GA8SA2 group increased, the area of the GA15SA5 group decreased, and the area of the GA10SA3 group was almost unchanged, which may be due to a mismatch in the rates of the swelling and degradation in which the hydrogel scaffolds during culture (Kaliampakou et al., 2023). Meanwhile, the cell survival rate of the scaffolds was above 88%. We established a well-established standard printing optimization process based on the rheological properties of hydrogels by comprehensively evaluating the print molding effect and chondrocyte activity of cell-loaded hydrogel scaffolds.

Designing hydrogel matrices with desirable mechanical properties as scaffolds for loading chondrocytes is key to cartilage tissue engineering. It has been found that hydrogels can influence matrix formation by chondrocytes through the synergistic effect of biochemical composition and mechanical properties. However, the appropriate mechanical stiffness to induce matrix secretion by chondrocytes varies depending on the composition of the hydrogel. For example, in bioprinted GelMA-HAMA hydrogel scaffolds, the ideal combination required for cartilage formation is the component ratio (2:1) and stiffness (30–60 kPa) (Martyniak et al., 2022). However, chondrocytes cultured in gelatin-hydroxyphenylpropionic acid hydrogels with a stiffness of 1,000 Pa were able to produce higher levels of sGAG (Wang et al., 2014). In a two-component

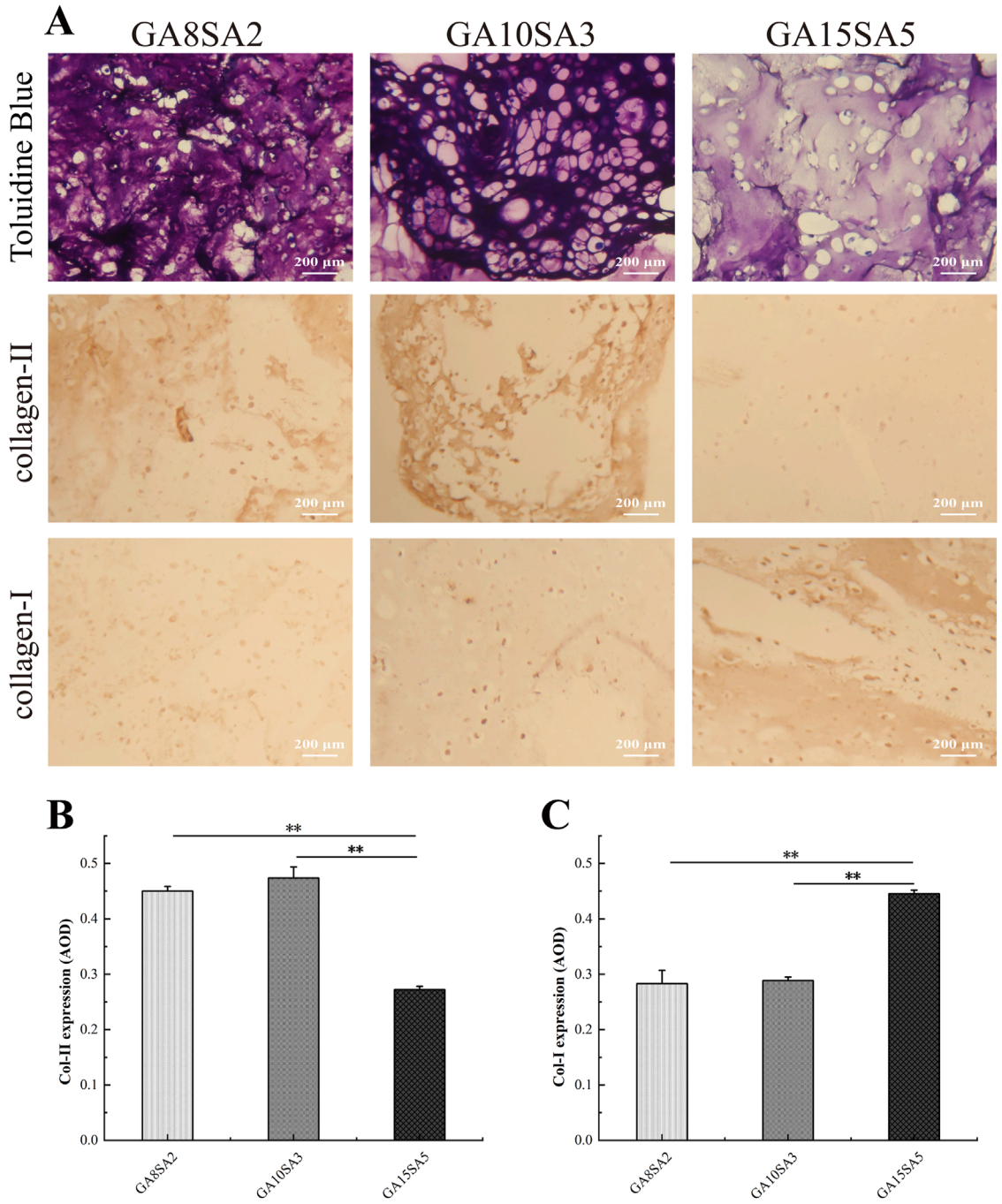

FIGURE 7
Histological evaluation of chondrocyte-loaded hydrogel scaffolds. **(A)** Light microscopic observation of hydrogel scaffolds after Toluidine blue staining and immunostaining. Quantitative analysis of the expression of Col-II **(B)** and Col-I **(C)**. Dates are represented as the mean ± SD (n = 3). Comparison between groups,$^{*}p < 0.05$,$^{**}p < 0.01$.

hydrogel based on chitosan and oxidized hyaluronic acid, the stiffer (~0.19 MPa) stiffness contributed to the formation of spherical aggregates and enhanced ECM expression by chondrocytes, whereas the softer (~0.13 MPa) stiffness exhibited good cell viability during the first 7 days of culture (Thomas et al., 2017). There are more mechanical parameters characterizing hydrogels in current studies investigating the interaction between matrix elasticity and chondrocyte behavior, including Young's modulus, equilibrium modulus, storage modulus, and shear stress and so on (Bachmann et al., 2020). However, it is difficult to make comparisons between studies due to the diversity and inconsistency of mechanical tests. Mechanical testing of constructs is usually performed before and after cell encapsulation and mainly characterizes the initial stiffness of the hydrogel. Among these, the storage

modulus is simpler to test and better characterizes the initial stiffness of the hydrogel. Other moduli, such as Young's modulus and aggregate modulus, provide further insight into the role of hydrogel mechanical properties in cartilage formation. Therefore, to determine the ideal combination of GA and SA for cartilage formation, we prepared and mechanically characterized three groups of GA-SA hydrogels with different concentrations (8:2, 10:3, and 15:5). The G′ of the hydrogels increased with the component ratio and showed a multiplicative relationship (~81.18 kPa, ~155.01 kPa and ~308.18 kPa). And G′ was the main determinant of the mechanical stiffness of hydrogel scaffolds (Cao et al., 2016), indicating that the mechanical stiffness of the three groups of hydrogel scaffolds was positively correlated with the proportion of hydrogel components. After the hydrogels loaded with chondrocytes were bioprinted to form the scaffolds, the hydrogels with low stiffness had good cellular activity (>92%), but the hydrogels with high stiffness affected the cellular activity (~88%). The hydrogel scaffolds were incubated for 21 d. Chondrocyte aggregation into spherical morphology was observed in GA8SA2 and GA10SA3 scaffolds at 14 d. Then, the number and size of chondrocyte spherical aggregates increased further at 21 d, and the GA10SA3 group outperformed the GA8SA2 group. This may be due to the increased gelatin component that promotes chondrogenesis within the stiffness range suitable for chondrocytes to maintain a transparent phenotype (Chameettachal et al., 2016). In the stiffer GA15SA5 group, chondrocytes consistently failed to form spherical aggregates, which could be the result of the higher stiffness. The results of RT-PCR also confirmed that compared with the GA15SA5 group, the hydrogel of the GA10SA3 group could better promote the expression of chondrogenesis-related genes (SOX9, Agg, Col-II). In further studies, we performed pathological staining and immunostaining of the hydrogel scaffolds in each group and found that the GA10SA3 group formed typical cartilage lacunae and showed a significant increase in the expression of type-II collagen and a decrease in the expression of type-I collagen compared with the other groups.

5 Conclusion

This study prepared GA-SA printed scaffolds with different component ratios and studied the effects of composition and mechanical stiffness on the activity and phenotype maintenance of chondrocytes. According to the rheological properties of hydrogels, a standard printing protocol of scaffolds was established. Moreover, the relationship between hydrogels with different composition ratio and stiffness and the formation of cartilage matrix was compared. It was revealed for the first time that the scaffold with the GA and SA component ratio (10:3) and mechanical stiffness (~155 kPa) has long-lasting morphological fidelity, effectively maintains the transparent phenotype of chondrocytes, and is more conducive to cartilage regeneration. Therefore, optimizing the composition and stiffness of hydrogels is a simple and effective means to promote chondrocyte proliferation and cartilage matrix production, thereby maximizing their potential to treat cartilage defects.

Data availability statement

The raw data supporting the conclusion of this article will be made available by the authors, without undue reservation.

Ethics statement

The animal study was approved by the Animal Ethics Committee of Affiliated Zhongshan Hospital of Dalian University. The study was conducted in accordance with the local legislation and institutional requirements.

Author contributions

GL: Data curation, Formal Analysis, Investigation, Methodology, Visualization, Writing–original draft, Writing–review and editing. XW: Formal Analysis, Supervision, Visualization, Writing–review and editing. JL: Formal Analysis, Supervision, Visualization, Writing–review and editing. YZ: Formal Analysis, Supervision, Visualization, Writing–review and editing. JZ: Data curation, Visualization, Writing–review and editing. MJ: Data curation, Visualization, Writing–review and editing. TG: Resources, Supervision, Visualization, Writing–review and editing. DZ: Funding acquisition, Project administration, Resources, Supervision, Writing–review and editing.

Funding

The author(s) declare that financial support was received for the research, authorship, and/or publication of this article. This work was supported by Dalian Dengfeng Plan Medical Key Specialty Construction Project (2021) No. 243 and Dalian University Interdisciplinary Projects (DLUXK-2023-QN-014).

Conflict of interest

The authors declare that the research was conducted in the absence of any commercial or financial relationships that could be construed as a potential conflict of interest.

Publisher's note

References

Abdollahiyan, P., Oroojalian, F., Mokhtarzadeh, A., and de la Guardia, M. (2020). Hydrogel-based 3D bioprinting for bone and cartilage tissue engineering. *Biotechnol. J.* 15 (12), e2000095. doi:10.1002/biot.202000095

Armiento, A. R., Alini, M., and Stoddart, M. J. (2019). Articular fibrocartilage - why does hyaline cartilage fail to repair? *Adv. Drug Deliv. Rev.* 146, 289–305. doi:10.1016/j.addr.2018.12.015

Bachmann, B., Spitz, S., Schädl, B., Teuschl, A. H., Redl, H., Nürnberger, S., et al. (2020). Stiffness matters: fine-tuned hydrogel elasticity alters chondrogenic redifferentiation. *Front. Bioeng. Biotechnol.* 8, 373. doi:10.3389/fbioe.2020.00373

Caddeo, S., Boffito, M., and Sartori, S. (2017). Tissue engineering approaches in the design of healthy and pathological *in vitro* tissue models. *Front. Bioeng. Biotechnol.* 5, 40. doi:10.3389/fbioe.2017.00040

Cao, Y., Lee, B. H., Peled, H. B., and Venkatraman, S. S. (2016). Synthesis of stiffness-tunable and cell-responsive Gelatin-poly(ethylene glycol) hydrogel for three-dimensional cell encapsulation. *J. Biomed. Mater Res. A* 104 (10), 2401–2411. doi:10.1002/jbm.a.35779

Chameettachal, S., Midha, S., and Ghosh, S. (2016). Regulation of chondrogenesis and hypertrophy in silk fibroin-gelatin-based 3D bioprinted constructs. *ACS Biomater. Sci. Eng.* 2 (9), 1450–1463. doi:10.1021/acsbiomaterials.6b00152

Chen, X. B., Fazel Anvari-Yazdi, A., Duan, X., Zimmerling, A., Gharraei, R., Sharma, N. K., et al. (2023). Biomaterials/bioinks and extrusion bioprinting. *Bioact. Mater* 28, 511–536. doi:10.1016/j.bioactmat.2023.06.006

Chung, J. H. Y., Naficy, S., Yue, Z., Kapsa, R., Quigley, A., Moulton, S. E., et al. (2013). Bio-ink properties and printability for extrusion printing living cells. *Biomater. Sci.* 1 (7), 763–773. doi:10.1039/c3bm00012e

Daly, A. C., and Kelly, D. J. (2019). Biofabrication of spatially organised tissues by directing the growth of cellular spheroids within 3D printed polymeric microchambers. *Biomaterials* 197, 194–206. doi:10.1016/j.biomaterials.2018.12.028

Duan, B., Hockaday, L. A., Kang, K. H., and Butcher, J. T. (2013). 3D bioprinting of heterogeneous aortic valve conduits with alginate/gelatin hydrogels. *J. Biomed. Mater Res. A* 101 (5), 1255–1264. doi:10.1002/jbm.a.34420

Fu, L., Li, P., Li, H., Gao, C., Yang, Z., Zhao, T., et al. (2021). The application of bioreactors for cartilage tissue engineering: advances, limitations, and future perspectives. *Stem Cells Int.* 2021, 1–13. doi:10.1155/2021/6621806

Gao, T., Gillispie, G. J., Copus, J. S., Pr, A. K., Seol, Y. J., Atala, A., et al. (2018). Optimization of gelatin-alginate composite bioink printability using rheological parameters: a systematic approach. *Biofabrication* 10 (3), 034106. doi:10.1088/1758-5090/aacdc7

Gao, Y., Gao, J., Li, H., Du, D., Jin, D., Zheng, M., et al. (2019). Autologous costal chondral transplantation and costa-derived chondrocyte implantation: emerging surgical techniques. *Ther. Adv. Musculoskelet. Dis.* 11, 1759720x19877131. doi:10.1177/1759720x19877131

Giuseppe, M. D., Law, N., Webb, B., R, A. M., Liew, L. J., Sercombe, T. B., et al. (2018). Mechanical behaviour of alginate-gelatin hydrogels for 3D bioprinting. *J. Mech. Behav. Biomed. Mater* 79, 150–157. doi:10.1016/j.jmbbm.2017.12.018

Gobbi, A., Lane, J. G., and Dallo, I. (2020). Editorial commentary: cartilage restoration-what is currently available? *Arthroscopy* 36 (6), 1625–1628. doi:10.1016/j.arthro.2020.04.001

Gregory, T., Benhal, P., Scutte, A., Quashie, D., Jr., Harrison, K., Cargill, C., et al. (2022). Rheological characterization of cell-laden alginate-gelatin hydrogels for 3D biofabrication. *J. Mech. Behav. Biomed. Mater* 136, 105474. doi:10.1016/j.jmbbm.2022.105474

Henrionnet, C., Pourchet, L., Neybecker, P., Messaoudi, O., Gillet, P., Loeuille, D., et al. (2020). Combining innovative bioink and low cell density for the production of 3D-bioprinted cartilage substitutes: a pilot study. *Stem Cells Int.* 2020, 1–16. doi:10.1155/2020/2487072

Kaliampakou, C., Lagopati, N., Pavlatou, E. A., and Charitidis, C. A. (2023). Alginate-gelatin hydrogel scaffolds; an optimization of post-printing treatment for enhanced degradation and swelling behavior. *Gels* 9 (11), 857. doi:10.3390/gels9110857

Kang, D., Liu, Z., Qian, C., Huang, J., Zhou, Y., Mao, X., et al. (2023). 3D bioprinting of a gelatin-alginate hydrogel for tissue-engineered hair follicle regeneration. *Acta Biomater.* 165, 19–30. doi:10.1016/j.actbio.2022.03.011

Katz, J. N., Arant, K. R., and Loeser, R. F. (2021). Diagnosis and treatment of hip and knee osteoarthritis: a review. *Jama* 325 (6), 568–578. doi:10.1001/jama.2020.22171

Kyburz, K. A., and Anseth, K. S. (2015). Synthetic mimics of the extracellular matrix: how simple is complex enough? *Ann. Biomed. Eng.* 43 (3), 489–500. doi:10.1007/s10439-015-1297-4

Lafuente-Merchan, M., Ruiz-Alonso, S., García-Villén, F., Gallego, I., Gálvez-Martín, P., Saenz-Del-Burgo, L., et al. (2022). Progress in 3D bioprinting technology for osteochondral regeneration. *Pharmaceutics* 14 (8), 1578. doi:10.3390/pharmaceutics14081578

Lee, K. Y., and Mooney, D. J. (2012). Alginate: properties and biomedical applications. *Prog. Polym. Sci.* 37 (1), 106–126. doi:10.1016/j.progpolymsci.2011.06.003

Lee, Y. B., Jeon, O., Lee, S. J., Ding, A., Wells, D., and Alsberg, E. (2021). Induction of 4D spatiotemporal geometric transformations in high cell density tissues via shape changing hydrogels. *Adv. Funct. Mater* 31 (24), 2010104. doi:10.1002/adfm.202010104

Liao, S., Meng, H., Zhao, J., Lin, W., Liu, X., Tian, Z., et al. (2022). Injectable adipose-derived stem cells-embedded alginate-gelatin microspheres prepared by electrospray for cartilage tissue regeneration. *J. Orthop. Transl.* 33, 174–185. doi:10.1016/j.jot.2022.03.007

Liu, B., Jin, M., and Wang, D. A. (2023a). *In vitro* expansion of hematopoietic stem cells in a porous hydrogel-based 3D culture system. *Acta Biomater.* 161, 67–79. doi:10.1016/j.actbio.2023.01.057

Liu, E., Zhu, D., Gonzalez Diaz, E., Tong, X., and Yang, F. (2021). Gradient hydrogels for optimizing niche cues to enhance cell-based cartilage regeneration. *Tissue Eng. Part A* 27 (13-14), 929–939. doi:10.1089/ten.TEA.2020.0158

Liu, G., Wei, X., Zhai, Y., Zhang, J., Li, J., Zhao, Z., et al. (2024). 3D printed osteochondral scaffolds: design strategies, present applications and future perspectives. *Front. Bioeng. Biotechnol.* 12, 1339916. doi:10.3389/fbioe.2024.1339916

Liu, Y., Yuan, Z., Liu, S., Zhong, X., Wang, Y., Xie, R., et al. (2023b). Bioactive phenylboronic acid-functionalized hyaluronic acid hydrogels induce chondro-aggregates and promote chondrocyte phenotype. *Macromol. Biosci.* 23 (11), e2300153. doi:10.1002/mabi.202300153

Martyniak, K., Lokshina, A., Cruz, M. A., Karimzadeh, M., Kemp, R., and Kean, T. J. (2022). Biomaterial composition and stiffness as decisive properties of 3D bioprinted constructs for type II collagen stimulation. *Acta Biomater.* 152, 221–234. doi:10.1016/j.actbio.2022.08.058

Morshedloo, F., Khoshfetrat, A. B., Kazemi, D., and Ahmadian, M. (2020). Gelatin improves peroxidase-mediated alginate hydrogel characteristics as a potential injectable hydrogel for soft tissue engineering applications. *J. Biomed. Mater Res. B Appl. Biomater.* 108 (7), 2950–2960. doi:10.1002/jbm.b.34625

Na, Y., Shi, Y., Liu, W., Jia, Y., Kong, L., Zhang, T., et al. (2019). Is implantation of autologous chondrocytes superior to microfracture for articular-cartilage defects of the knee? A systematic review of 5-year follow-up data. *Int. J. Surg.* 68, 56–62. doi:10.1016/j.ijsu.2019.06.007

Naghieh, S., and Chen, X. (2021). Printability-A key issue in extrusion-based bioprinting. *J. Pharm. Anal.* 11 (5), 564–579. doi:10.1016/j.jpha.2021.02.001

Ojansivu, M., Rashad, A., Ahlinder, A., Massera, J., Mishra, A., Syverud, K., et al. (2019). Wood-based nanocellulose and bioactive glass modified gelatin-alginate bioinks for 3D bioprinting of bone cells. *Biofabrication* 11 (3), 035010. doi:10.1088/1758-5090/ab0692

Rahimnejad, M., Labonté-Dupuis, T., Demarquette, N. R., and Lerouge, S. (2020). A rheological approach to assess the printability of thermosensitive chitosan-based biomaterial inks. *Biomed. Mater* 16 (1), 015003. doi:10.1088/1748-605X/abb2d8

Redondo, M. L., Beer, A. J., and Yanke, A. B. (2018). Cartilage restoration: microfracture and osteochondral autograft transplantation. *J. Knee Surg.* 31 (3), 231–238. doi:10.1055/s-0037-1618592

Salzmann, G. M., Ossendorff, R., Gilat, R., and Cole, B. J. (2021). Autologous minced cartilage implantation for treatment of chondral and osteochondral lesions in the knee joint: an overview. *Cartilage* 13 (1_Suppl. l), 1124s–1136s. doi:10.1177/1947603520942952

Schwab, A., Levato, R., D'Este, M., Piluso, S., Eglin, D., and Malda, J. (2020). Printability and shape fidelity of bioinks in 3D bioprinting. *Chem. Rev.* 120 (19), 11028–11055. doi:10.1021/acs.chemrev.0c00084

Seo, Y., Lee, H., Lee, J. W., and Lee, K. Y. (2019). Hyaluronate-alginate hybrid hydrogels prepared with various linkers for chondrocyte encapsulation. *Carbohydr. Polym.* 218, 1–7. doi:10.1016/j.carbpol.2019.04.067

Skardal, A., and Atala, A. (2015). Biomaterials for integration with 3-D bioprinting. *Ann. Biomed. Eng.* 43 (3), 730–746. doi:10.1007/s10439-014-1207-1

Thomas, V. T., Vg, R., and P, D. N. (2017). Effect of stiffness of chitosan-hyaluronic acid dialdehyde hydrogels on the viability and growth of encapsulated chondrocytes. *Int. J. Biol. Macromol.* 104 (Pt B), 1925–1935. doi:10.1016/j.ijbiomac.2017.05.116

Wang, H., Zhang, J., Liu, H., Wang, Z., Li, G., Liu, Q., et al. (2023). Chondrocyte-laden gelatin/sodium alginate hydrogel integrating 3D printed PU scaffold for auricular cartilage reconstruction. *Int. J. Biol. Macromol.* 253 (Pt 1), 126294. doi:10.1016/j.ijbiomac.2023.126294

Wang, L. S., Du, C., Toh, W. S., Wan, A. C., Gao, S. J., and Kurisawa, M. (2014). Modulation of chondrocyte functions and stiffness-dependent cartilage repair using an injectable enzymatically crosslinked hydrogel with tunable mechanical properties. *Biomaterials* 35 (7), 2207–2217. doi:10.1016/j.biomaterials.2013.11.070

Wu, Z., Li, Q., Xie, S., Shan, X., and Cai, Z. (2020). *In vitro* and *in vivo* biocompatibility evaluation of a 3D bioprinted gelatin-sodium alginate/rat Schwann-cell scaffold. *Mater Sci. Eng. C Mater Biol. Appl.* 109, 110530. doi:10.1016/j.msec.2019.110530

Yasui, Y., Wollstein, A., Murawski, C. D., and Kennedy, J. G. (2017). Operative treatment for osteochondral lesions of the talus: biologics and scaffold-based therapy. *Cartilage* 8 (1), 42–49. doi:10.1177/1947603516644298

Zhang, J., Wehrle, E., Adamek, P., Paul, G. R., Qin, X. H., Rubert, M., et al. (2020). Optimization of mechanical stiffness and cell density of 3D bioprinted cell-laden scaffolds improves extracellular matrix mineralization and cellular organization for bone tissue engineering. *Acta Biomater.* 114, 307–322. doi:10.1016/j.actbio.2020.07.016

Zhang, L., Yang, G., Johnson, B. N., and Jia, X. (2019). Three-dimensional (3D) printed scaffold and material selection for bone repair. *Acta Biomater.* 84, 16–33. doi:10.1016/j.actbio.2018.11.039

Zhang, Q., Deng, S., Sun, K., Lin, S., Lin, Y., Zhu, B., et al. (2017). MMP-2 and Notch signal pathway regulate migration of adipose-derived stem cells and chondrocytes in co-culture systems. *Cell. Prolif.* 50 (6), e12385. doi:10.1111/cpr.12385

Zhao, Y., Li, Y., Mao, S., Sun, W., and Yao, R. (2015). The influence of printing parameters on cell survival rate and printability in microextrusion-based 3D cell printing technology. *Biofabrication* 7 (4), 045002. doi:10.1088/1758-5090/7/4/045002

Zhou, Z., Zheng, J., Meng, X., and Wang, F. (2023). Effects of electrical stimulation on articular cartilage regeneration with a focus on piezoelectric biomaterials for articular cartilage tissue repair and engineering. *Int. J. Mol. Sci.* 24 (3), 1836. doi:10.3390/ijms24031836